Transferable Ordered Ni Hollow Sphere Arrays Induced by Electrodeposition on Colloidal Monolayer

Guotao Duan, Weiping Cai,* Yue Li, Zhigang Li, Bingqiang Cao, and Yuanyuan Luo

Key Lab of Materials Physics, Anhui Key Lab of Nanomaterials and Nanotechnology, Institute of Solid State Physics, Chinese Academia of Sciences, Hefei, 230031, Anhui, P. R. China

Received: December 21, 2005; In Final Form: February 5, 2006

We report an electrochemical synthesis of two-dimensionally ordered porous Ni arrays based on polystyrene sphere (PS) colloidal monolayer. The morphology can be controlled from bowl-like to hollow sphere-like structure by changing deposition time under a constant current. Importantly, such ordered Ni arrays on a conducting substrate can be transferred integrally to any other desired substrates, especially onto an insulting substrate or curved surface. The magnetic measurements of the two-dimensional hollow sphere array show the coercivity values of 104 Oe for the applied field parallel to the film, and 87 Oe for the applied field perpendicular to the film, which is larger than those of bulk Ni and hollow Ni submicrometer-sized spheres. The formation of hollow sphere arrays is attributed to preferential nucleation on the interstitial sites between PS in the colloidal monolayer and substrate, and growth along PSs' surface. The transferability of the arrays originates from partial contact between the Ni hollow spheres and substrate. Such novel Ni ordered nanostructured arrays with transferability and high magnetic properties should be useful in applications such as data storage, catalysis, and magnetics.

1. Introduction

Two-dimensionally (2D) ordered porous arrays based on the colloidal monolayer have received considerable attention in recent years[1−13] due to their unique properties and potential applications in catalysis,[1] photonic crystals,[14] optoelectronic devices,[15] surface-enhanced Raman spectroscopy (SERS),[16,17] enhanced optical transmission,[18] and cell cultures.[2] There are many methods available for the production of the porous arrays based on the colloidal monolayer, such as, spray pyrolysis,[1] sol−gel,[2] solution-dipping,[8] and electrochemical deposition techniques.[7,9] The pores in the arrays can assume diverse morphologies, such as bowl-like,[11] wall-like,[10] and hollow sphere.[3,12,13] Obviously, it is very important to synthesize the ordered porous arrays with controlled morphology. As we know, Ni-based nanomaterials have important physical properties and potential applications in the fields of catalysts,[19] high-density data storage,[20] electrodes,[21] and sensors.[22] Preparation of morphology-controlled ordered Ni porous array should be of importance both in fundamental research, such as, their morphology-dependent electric and magnetic properties, and also in applications. Electrochemical deposition is a facile and low-cost method and can be used in industry. The formation of nanostructured array using electrochemical methods can easily be controlled through adjusting deposition parameters. In this paper, we report the synthesis of ordered porous Ni arrays using an electrochemical deposition strategy based on polystyrene sphere (PS) colloidal monolayer. The morphology can be controlled from a bowl-like to a hollow sphere-like structure just by changing deposition time at a constant deposition current. Importantly, such ordered porous (including hollow sphere) Ni arrays on a conducting substrate can be transferred integrally to any other desired substrates, especially onto an insulating substrate or curved surface. Such transferability can avoid restriction of electro-deposition to conductive substrates, making it very flexible to fabricate such ordered arrays on any desired substrates including insulating or adiabatic substrate, which is beneficial to study electronic transportation, magnetics, electromagnetics, and heat exchange for this film. In addition, this 2D ordered Ni hollow sphere arrays with transferability have exhibited novel magnetic properties and applications. The details are reported in this article.

2. Experimental Section

The PS (1000 nm in diameter) suspensions were bought from Alfa Aesar Corporation. Glass substrates were cleaned according to Dyune's procedures.[23] The square centimeter sized ordered PS colloidal monolayer was fabricated on the glass substrates by spin-coating method on a custom-built spin-coater. Some ITO-glass substrates were ultrasonically cleaned in acetone, ethanol, and distilled water for 30 min each. The monolayer on the glass substrate was integrally lifted off and floated on the surface of distilled water in a cup, and then picked up with an ITO glass, as illustrated previously,[8] followed by heating at 110 °C in an oven for 2 min. The edges of the monolayer on the ITO-glass were covered by an aluminum frame and insulating tape, and immersed into an electrolyte solution as a working electrode. The electrolyte was prepared with 0.01M $NiCl_2$ and 0.03M $(NH_4)_2SO_4$, and its pH value was adjusted to 8 with ammonia. A polycrystalline clean nickel sheet was used as the auxiliary electrode. The distance between the working electrode and the auxiliary electrode was about 6 cm. The electrodeposition was carried out at 60 °C for a certain time. After deposition, the monolayer was removed by dissolving in CH_2Cl_2, and ordered arrays were thus obtained. Figure 1 schematically demonstrates fabrication of the nanostructured arrays.

The morphologies of the samples were examined on a Sirion 200 field-emission scanning electronic microscope (FESEM).

* To whom all correspondence should be addressed. E-mail: wpcai@issp.ac.cn.

10.1021/jp057421t CCC: $33.50
Published on Web 03/23/2006

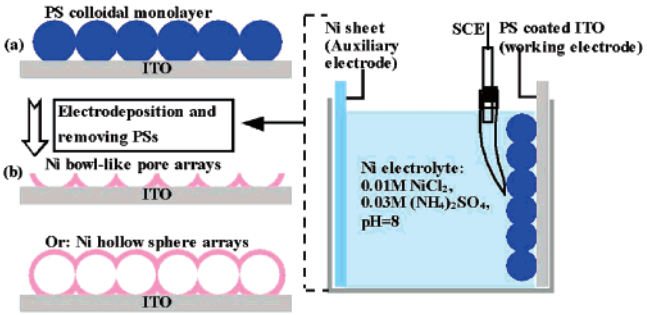

Figure 1. Schematic electrodeposition procedures based on PS colloidal monolayer. (a) Colloidal monolayer sintered on the ITO-glass substrate by heating. (b) Ordered bowl-like pore arrays or hollow sphere arrays after electrodeposition for a short time or a long time and removal of the monolayer. The right: electrodeposition in a custom-built cell.

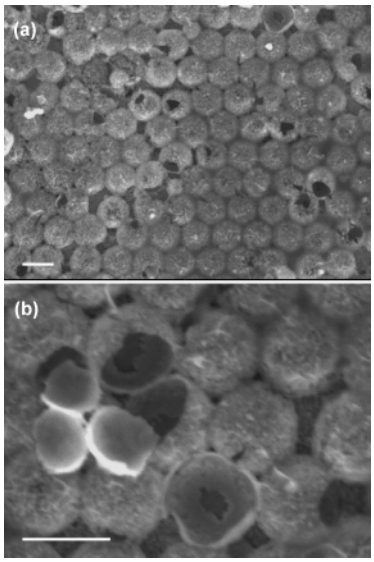

Figure 2. FESEM images of the as-deposited sample after removal of the colloidal monolayer. The sample was electrodeposited for 90 min at cathodic deposition current density 0.25mA/cm^2. Scale bars are 1 μm. (b) is a local magnification of (a).

X-ray diffraction (XRD) was measured on the Philips X'Pert using Cu Kα line (0.15419 nm). Room temperature (300K) hysteresis loop measurements of the samples were obtained by superconducting quantum interference device (SQUID) magnetometer.

3. Results and Discussion

3.1. Hollow Sphere Arrays. By a spin-coating method, large-area monolayer colloidal crystals (>1 cm^2),with a hexagonally close-packed arrangement, were fabricated on a glass substrate successfully, and the whole monolayer film is composed of many ordered domains with size ranging from several tens to hundreds of square micrometers, as illustrated previously.[13,24] Such a colloidal monolayer was then transferred to the ITO-glass substrate and heated, followed by electro-deposition. Figure 2 shows the morphology of the sample after deposition for 90 min at a low current density (0.25mA/cm^2) and removal of the PS template. The hollow sphere arrays are formed. We can estimate the thickness of the sphere shell to be about 60 nm from these broken hollow spheres. Corresponding XRD measurement has confirmed that the as-prepared hollow sphere arrays are nickel crystal with face-centered cubic lattice structure, as shown in Figure 3. It has been revealed that the deposition time is important to formation of the hollow sphere

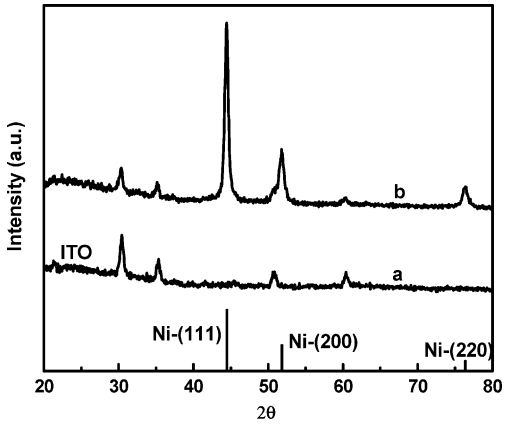

Figure 3. XRD patterns for the as-deposited samples and ITO. (a) ITO, (b) the sample shown in Figure 2. Bottom: standard diffraction of Ni powders.

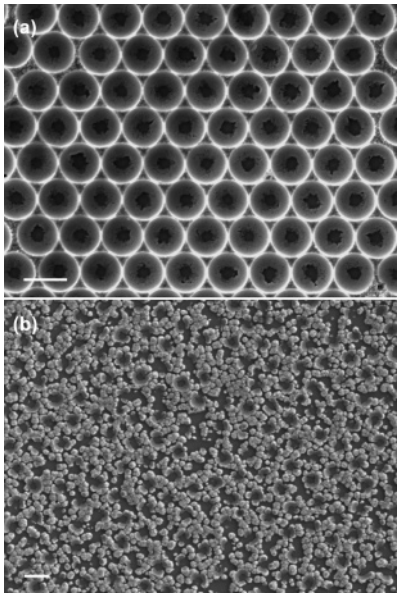

Figure 4. FESEM images of the as-deposited samples at current density 0.25mA/cm^2 after removal of the colloidal monolayer. The electrodeposition time was, respectively, (a) 45min and (b) 15min. Both scale bars are 1 μm.

arrays under the constant current. If the deposition time is decreased to 45 min, morphology of the sample evolves from a hollow sphere to a bowl-like structure (see Figure 4a). When deposition time is further decreased to 15min, only nearly spherical nanoparticles were obtained on the substrate (see Figure 4b).

More interestingly, such ordered hollow sphere arrays and bowl-like ordered porous arrays can be removed integrally from the ITO-glass substrate by immersion into water, which floats on the water surface, and then transferred integrally to another new substrate by picking it up with a desired substrate, as shown in Figure 5. The new substrate could be an insulating material with flat or even curved surface. Such transferability of the film is of importance because we can avoid restriction of electro-deposition to conductive substrate, and make it very flexible to fabricate such ordered pore or hollow sphere arrays on any desired substrates with flat or even curved surface. In addition, based on such transferability, we can also examine the morphology of the backside of the film (or the array) by turning over the floating film during picking it up. Figure 6 exhibits the backside morphology of the hollow sphere arrays on a silicon substrate by such transferring. The dark contrast pore-like

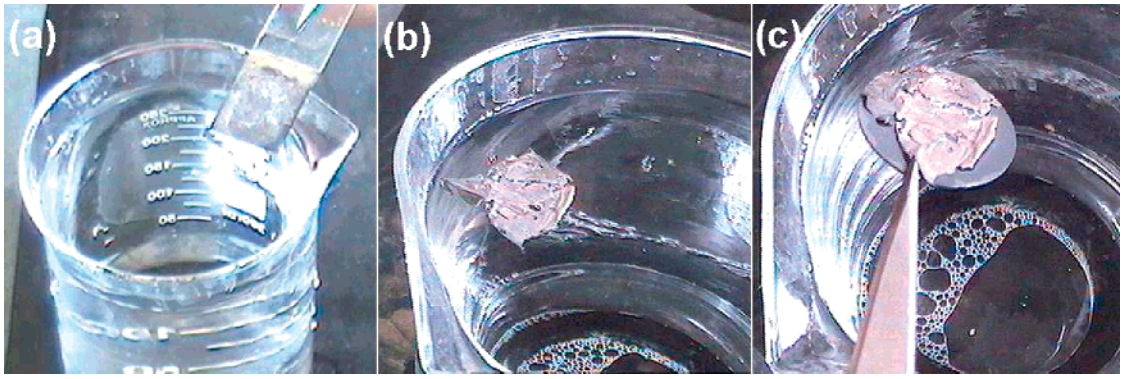

Figure 5. Photos depicting transferring a Ni hollow sphere array on ITO substrate to a silicon substrate. (a) The hollow sphere array on ITO-glass, (b) lift-off in water, (c) pick-up of the array with a silicon substrate.

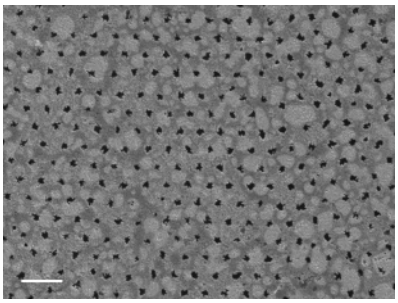

Figure 6. FESEM image of the backside of the film, shown in Figure 2, on silicon substrate. Scale bar is 2 μm.

structure originates from the heating-induced planar contact of PSs with substrate.

Further experiments demonstrate that the cathodic deposition current density is crucial to the formation of such arrays and their transferability. When the current density is increased to 1.0mA/cm^2, the bowl-like ordered porous arrays can still be formed after a short deposition time (12 min for instance) but are un-transferable, while hollow sphere arrays cannot be obtained after increasing deposition time (see Figure 7a). A middle current density of 0.4mA/cm^2 leads to a transition morphology and un-transferable film. Hollow spherical structure is formed after a long deposition time (60 min), however, the spherical shell is incompact (see Figure 7b).

The formation of the hollow sphere arrays can easily be understood. Based on Figure 4b, we know that Ni nuclei were preferentially formed at the bottom interstitial sites between PSs and the substrate (see the solid arrow in Figure 8) and then grew along PSs' surface during deposition at a low cathodic deposition current density, forming bowl-like ordered porous arrays after shorter deposition, or hollow sphere arrays after longer deposition, as seen in Figure 4a and Figure 2, or the left column of Figure 8. In our case, the PSs are surface negatively charged, which induces the Ni^{2+} ion (existing in the form of $[Ni(NH_3)_2]^{2+}$)[25] to adsorb on the PSs' surface easily. Thus, PSs' surface should be of lower barrier for Ni nucleation and growth compared with ITO substrate, leading to the preferential nucleation and growth on the PSs. Due to such preferential nucleation and growth along PSs' surface, there will exist small interstitials between the deposited film and the substrate, meaning partial contact between the film and the substrate. So the adherence force between substrate and the Ni film (or array) is weak enough for such film to be removed by water surface tension in water, leading to transferability.

As we know, high current density should correspond to a high deposition rate, which will result in homogeneous (or unselective) nucleation on the substrate. Obviously, when the thickness of a deposition film is smaller than the PSs' radius (after a short deposition time), bowl-like pore morphology would always be formed due to the PSs' geometry, irrespective of current density. For the film with a thickness larger than the PSs' radius (after a longer deposition time), however, high deposition current density will lead to failure to the preferential growth surrounding PSs' surface; hence, the hollow spherical shell will not be formed, as illustrated in Figure 7a and the right column of Figure 8. In addition, due to unselective nucleation on the substrate, the deposited film will contact fully with the substrate, leading to an increase of the adherence force between them. In this case, the film cannot be removed integrally by the surface tension in water. Thus, a middle current density (0.4 mA/cm^2) induces a transition between the two modes above (the un-selective nucleation on the substrate and preferential growth along PSs) or coexistence of them. A hollow spherical shell is still formed due to preferential growth along PSs, while unselective nucleation on the substrate leads to un-transferability (see Figure 7b).

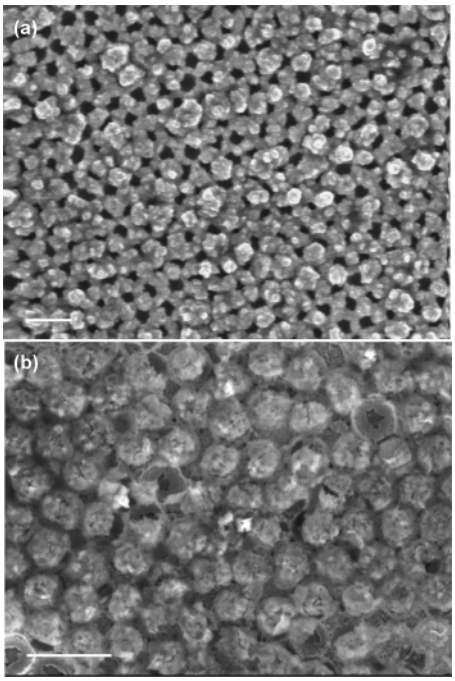

Figure 7. FESEM images of the samples electrodeposited for (a) 25min at cathodic current density $J = 1.0$ mA/cm^2 and (b) 60 min at $J = 0.4$ mA/cm^2 based on PS monolayer. Both scale bars are 2 μm.

3.2. Magnetic Measurements. Figure 9 shows the magnetic hysteresis loops of the 2D hollow sphere array shown in Figure 2. The coercivity (H_c) and remanence (M_r/M_s) for such array

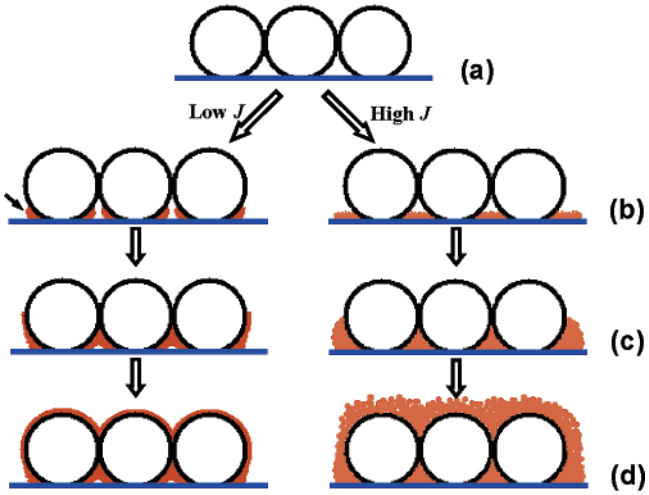

Figure 8. Schematic illustrations of the formation processes of ordered porous Ni arrays at different cathodic current density (*J*). (a) colloidal monolayer sintered on the ITO-glass substrate by heating, (b) Ni nucleation, (c) after a short deposition time, and (d) after a longer deposition time.

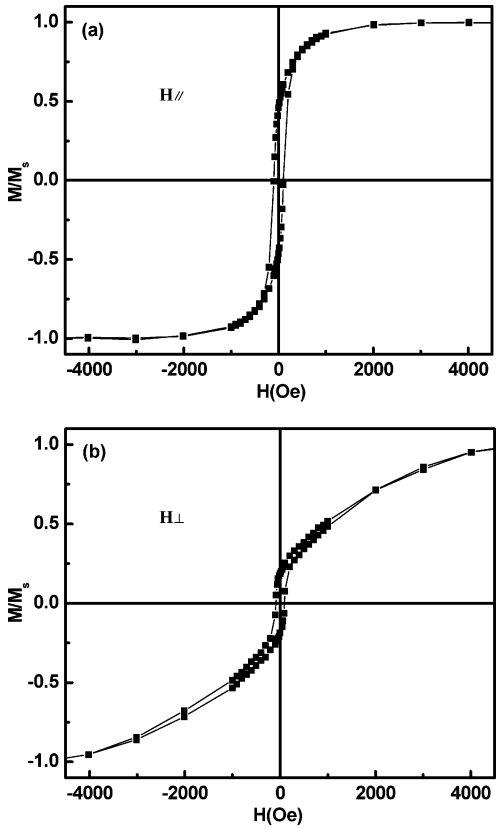

Figure 9. Hysteresis loops of the sample shown in Figure 2 at room temperature under the applied field parallel (a) or perpendicular (b) to the film plane.

is, respectively, 104 Oe and 0.46 under the applied field parallel to the film, and 87 Oe and 0.19 under the applied field perpendicular to the film. The coercivity is considerably larger than that for bulk Ni (H_c = 0.7 Oe) and hollow Ni submicrometer-sized sphere powers (H_c = 32.3 Oe),[26] and equal to that for hollow Ni nanometer-sized sphere powders (H_c = 102 Oe).[27] The M_r/M_s contrast for different orientations of applied fields is much smaller than that of the electrodeposited Ni film (M_r/M_s = 0.67 and 0.02 for the applied magnetic fields parallel and perpendicular to the film plane, respectively),[28] and close to that of 3D ordered Ni replicas on substrate (M_r/M_s = 0.35 and 0.10).[28]

The increase of coercivity for such hollow sphere array should be associated with its structure. A similar increase of coercivity was reported for 2D ferromagnetic network structures and 3D ordered Ni replicas, which was attributed to domain wall pinning by the network structure.[28−30] In our case, the network-like structure of the arrays and thin hollow spherical shell can easily lead to domain wall pinning,[28] and thus enhancement of the coercivity.

As previously reported,[28] Ni exhibits only a small magnetocrystalline anisotropy. Thus the magnetic response should be dominated by the shape anisotropy. The electrodeposited Ni film[28] is of strong shape anisotropy and, hence, exhibits high remanence (M_r/M_s = 0.67) characteristic of the easy-magnetized axis under the applied field parallel to the film plane, and a very low remanence (smaller than 0.02) characteristic of the hard magnetized axis under the applied field perpendicular to the film plane. Comparatively, the Ni hollow sphere array, in our case, shows a much smaller contrast of the remanences, indicating that the 2D ordered hollow sphere arrays are much more isotropic in magnetic response than the electrodeposited film. This can be attributed to the isotropic spherical structure of the single cells in the arrays although the whole arrays are two-dimensional. Both remanences, in our case, are larger than the corresponding values of the 3D Ni replicas, showing that the structure of the hollow sphere arrays is more easily magnetized.

4. Conclusions

In summary, by an electrochemical deposition strategy based on a PS colloidal monolayer, we have demonstrated the synthesis of 2D ordered bowl-like pore and hollow sphere-like Ni arrays, depending on the deposition time under constant current. In a certain deposition condition, preferential nucleation on the interstitial sites between PSs and substrate, and growth along PSs' surface will occur, resulting in the formation of Ni hollow sphere arrays, which only partially contact with the substrate and, hence, possess weak adherence force between them leading to its integral transferability in water. Such transferability of the film can avoid restriction of electrodeposition to conductive substrates, and make it very flexible to fabricate such ordered pore or hollow sphere arrays on any desired substrates with a flat or even a curved surface. It could also be beneficial to study the physical properties of the porous arrays, such as, electronic transport, magnetics, and heat exchange. Also, the 2D hollow sphere arrays show a high coercivity value, due to domain wall pinning induced by the network-like structure of the arrays and the thin hollow spherical shell, and low magnetic anisotropy due to the isotropic spherical structure of the single cells in the arrays.

Acknowledgment. The authors acknowledge the financial supports from the Natural Science Foundation of China (grant no: 50502032), and National Project for Basic Research (grant no. 2006CB300402).

References and Notes

(1) Matsushita, S. I.; Miwa, T.; Tryk, D. A.; Fujishima, A. *Langmuir* **1998**, *14*, 6441.
(2) Tatsuma, T.; Ikezawa, A.; Ohko, Y.; Miwa, T.; Matsue, T.; Fujishima, A. *Adv. Mater.* **2000**, *12*, 643.
(3) Han, S.; Shi, X.; Zhou, F. *Nano Lett.* **2002**, *2*, 97.
(4) Che, X.; Chen, Z.; Fu, N.; Lu, G.; Yang, B. *Adv. Mater.* **2003**, *15*, 1413.

(5) Yi, D. K.; Kim, D.-Y. *Nano lett.* **2003**, *3*, 207.
(6) Kanungo, M.; Collinson, M. M. *Chem. Commun.* **2004**, 548.
(7) Bartlett, P. N.; Baumberg, J. J.; Coyle, S.; Abdelsalam, M. E. *Faraday Discuss.* **2004**, *125*, 117.
(8) Sun, F.; Cai, W.; Li, Y.; Cao, B.; Lei, Y.; Zhang, L. *Adv. Funct. Mater*. **2004**, *14*, 283.
(9) Sun, F.; Cai, W.; Li, Y.; Cao, B.; Lu, F.; Duan, G.; Zhang, L. *Adv. Mater*. **2004**, *16*, 1116.
(10) Cao, B.; Cai, W.; Sun, F.; Li, Y.; Lei, Y.; Zhang, L. *Chem. Commun.* **2004**, 1604.
(11) Wang, X.; Graugnard, E.; King, J. S.; Wang, Z.; Summers, C. J. *Nano Lett.* **2004**, *4*, 2223.
(12) Chen, Z.; Zhan, P.; Wang, Z.; Zhang, J.; Zhang, W.; Ming, N.; Chan, C.; Sheng, P. *Adv. Mater.* **2004**, *16*, 417.
(13) Li, Y.; Cai, W.; Duan, G.; Cao, B.; Sun, F. *J. Mater. Res.* **2005**, *20*, 338.
(14) Birner, A.; Gruning, U.; Ottow, S.; Schneider, A.; Müller, F.; Lehmann, V.; Föll, H.; Gösele, U. *Phys. Status Solidi A* **1998**, *165*, 111.
(15) Imada, M.; Noda, S.; Chutinan, A.; Tokuda, T.; Murata, M.; Sasaki, G. *Appl. Phys. Lett.* **1999**, *75*, 316.
(16) Tessier, P. M.; Velev, O. D.; Kalambur, A. T.; Rabolt, J. F.; Lenhoff, A. M.; Kaler, E. W. *J. Am. Chem.* Soc. **2000**, *122*, 9554.
(17) Tessier, P. M.; Velev, O. D.; Kalambur, A. T. *Adv. Mater*. **2001**, *13*, 396.
(18) Ebbesen, T. W.; Lezec, H. J.; Ghaemi, H. F.; Thio, T.; Wolff, P. A. *Nature* **1998**, *391*, 667.
(19) Huang, Z.; Carnahan, D. L.; Rybczynski, J.; Giersig, M.; Sennett, M.; Wang, D.; Wen, J.; Kempa, K.; Ren, Z. *Appl. Phys. Lett.* **2003**, *82*, 460.
(20) Maya, L.; Thundat, T.; Thompson, J. R.; Stevenson, R. J. *Appl. Phys. Lett.* **1995**, *67*, 3034.
(21) Tai, Y.-L.; Teng, H. *Chem. Mater*. **2004**, *16*, 338.
(22) Walter, E. C.; Penner, R. M.; Liu, H.; Ng, K. H.; Zach, M. P.; Favier, F. *Surf. Interface Anal.* **2002**, *34*, 409.
(23) Haynes, C. L.; Van Duyne, R. P. *J. Phys. Chem. B* **2001**, *105*, 5599.
(24) Li, Y.; Cai, W.; Duan, G.; Sun, F.; Cao, B.; Lu, F.; Fang, Q.; Boyd, I. W. *Appl. Phys. A* **2005**, *81*, 269.
(25) Natarajan, C.; Matsumoto, H.; Nogami, G. *J. Electrochem. Soc.* **1995**, *144*, 121.
(26) Bao, J.; Liang, Y.; Xu, Z.; Si, L. *Adv. Mater.* **2003**, *15*, 1832.
(27) Liu, Q.; Liu, H.; Han, M.; Zhu, J.; Liang, Y.; Xu, Z.; Song, Y. *Adv. Mater.* **2005**, *17*, 1995.
(28) Eagleton, T. S.; Searson, P. C. *Chem. Mater.* **2004**, *16*, 5027.
(29) Liu, K.; Baker, S. M.; Tuominen, M.; Russell, T. P.; Schuller, I. K. *Phys. Rev. B* **2001**, *63*, 060403.
(30) Sun, L.; Ding, Y.; Chien, C. L.; Searson, P. C. *Phys. Rev. B* **2001**, *64*, 184430.